sustainability

MDPI

Article

Mitigation of Alkali–Silica Reactivity of Greywacke Aggregate in Concrete for Sustainable Pavements

Kinga Dziedzic, Aneta Brachaczek, Dominik Nowicki and Michał A. Glinicki *

Institute of Fundamental Technological Research, Polish Academy of Sciences, Pawinskiego St. 5B, 02-106 Warsaw, Poland; kdzie@ippt.pan.pl (K.D.); aantolik@ippt.pan.pl (A.B.); dnowicki@ippt.pan.pl (D.N.)
* Correspondence: mglinic@ippt.pan.pl

Abstract

Quality requirements for mineral aggregate for concrete used to construct pavement for busy highways are high because of the fatigue traffic loads and environmental exposure. The use of local aggregate for infrastructure projects could result in important sustainability improvements, provided that the concrete's durability is assured. The objective of this study was to identify the potential alkaline reactivity of local greywacke aggregate and select appropriate mitigation measures against the alkali–silica reaction. Experimental tests on concrete specimens were performed using the miniature concrete prism test at 60 °C. Mixtures of coarse greywacke aggregate up to 12.5 mm with natural fine aggregate of different potential reactivity were evaluated in respect to the expansion, compressive strength, and elastic modulus of the concrete. Two preventive measures were studied—the use of metakaolin and slag-blended cement. A moderate reactivity potential of the greywacke aggregate was found, and the influence of reactive quartz sand on the expansion and instability of the mechanical properties of concrete was evaluated. Both crystalline and amorphous alkali–silica reaction products were detected in the cracks of the greywacke aggregate. Efficient expansion mitigation was obtained for the replacement of 15% of Portland cement by metakaolin or the use of CEM III/A cement with the slag content of 52%, even if greywacke aggregate was blended with moderately reactive quartz sand. It resulted in a relative reduction in expansion by 85–96%. The elastic modulus deterioration was less than 10%, confirming an increased stability of the elastic properties of concrete.

Keywords: alkali-silica reaction; aggregate; concrete; metakaolin; highway pavement

Academic Editors: Chaohui Wang, Qian Chen, Ping Li and Yuanzhao Chen

Received: 18 June 2025
Revised: 15 July 2025
Accepted: 24 July 2025
Published: 27 July 2025

Citation: Dziedzic, K.; Brachaczek, A.; Nowicki, D.; Glinicki, M.A. Mitigation of Alkali–Silica Reactivity of Greywacke Aggregate in Concrete for Sustainable Pavements. *Sustainability* **2025**, *17*, 6825. https://doi.org/10.3390/su17156825

1. Introduction

Pavement for busy roads in Central Europe is often constructed using two-lift cement concrete paving technology with exposed aggregate surface [1,2]. Such pavement construction offers enhanced skidding resistance and ride comfort for the top layer while allowing for less stringent material specifications for the bottom layer. The flexibility of material selection for paving is very much desired, especially in respect to mineral aggregates that constitute more than 3/4 of cement concrete volume [3]. For instance, in Belgium the recycled concrete aggregates are allowed to replace up to 20% of coarse rock aggregates [1]. In the face of the depletion of good-quality mineral resources, there is a need to explore alternative local resources and, if necessary, seek material modifications that improve their quality [4,5]. Infrastructure projects, due to their size, consume a significant portion of natural rock aggregates, ca. 20,000 tons per kilometer of highway. In addition, transport of good-quality aggregates to areas where they are not available is costly and has an

additional negative environmental impact [6,7]. The potential savings from using local aggregate resources, both environmentally and economically friendly, are particularly worthy of investigation.

Crushed aggregate produced from greywacke rock is commonly used in asphalt concrete but could also be a valuable constituent of cement concrete for pavements, including the top layer of two-layer pavements with exposed aggregate. Their potential usefulness is indicated by the high resistance to polishing (PSV as per EN 1097-8 [8] of about 50), high resistance to abrasion (MDE as per EN 1097-1 [9] of about 20), and high resistance to fragmentation (LA as per EN 1097-2 [10] of about 20). According to the technical specifications of the Polish highway administration (GDDKiA) [11], coarse aggregates with PSV $\geq$ 50 and LA $\leq$ 25 meet the requirements for concrete constituents in the top layer of two-layer pavements on roads with the highest traffic load category. However, the durability of greywacke aggregate in concrete, particularly its resistance to alkali–silica reaction (ASR), raises doubts due to the presence of potentially reactive minerals [12,13]. The reactivity of locally quarried greywacke aggregate in concrete used for the construction of the Mactaquac Dam in New Brunswick, Canada, is known to be responsible for the substantial expansion and damage observed in the structure [14]. The first signs of ASR in concrete structures containing greywacke aggregate could be observed after 10 years of use, which classifies greywacke as a slow-reactive aggregate [12].

The use of local greywacke aggregates in concrete may require appropriate material modifications to reduce the destructive effects of ASR on pavement performance. While limiting the expansion of highly reactive aggregates and using them in concrete for infrastructure projects may be too risky, slow-reacting aggregates like greywacke, combined with inhibiting agents, could be an attractive alternative to non-reactive aggregates. Concrete blocks with greywacke aggregate and 25% fly ash addition showed no signs of reaction after 14 years of exposure and a reduction in concrete expansion in the laboratory from 1.6 to 0.05% after 3 years of testing [15]. Unlike flint, greywacke did not show a pessimum effect. Other mitigation measures like additions of $LiNO_3$ [16] and metakaolin [17] have been studied. A reduced limit on the permitted alkali content in concrete with greywacke, from 4.5 kg/m^3 to 3.5 kg/m^3 in the Irish recommendations [18], was also used as a mitigation measure.

The selection of fine aggregate and the resulting concrete mix workability is quite important from the perspective of slip-form construction technology and the desired precision of pavement finishing operations [1]. The practical significance of the potential reactivity of quartz sand is often discussed in the industry. Because the alkaline reactivity of coarse and fine aggregate fractions is classified separately there is a gap in the proper recognition of local fine and coarse aggregate blends.

The objective of this study was to identify the potential reactivity of local greywacke aggregate and select appropriate ASR mitigation measures. The scope of the investigation included evaluating mixtures of coarse greywacke aggregate with natural fine aggregate of different potential reactivity, aiming to increase the use of local mineral resources. Using the miniature concrete prism test (MCPT) the amount of ASR inhibiting additives was established, taking into account the influence of both coarse and fine aggregate on the expansion and mechanical properties of concrete.

2. Materials and Methods

2.1. Materials

Two locally quarried greywacke aggregates (denoted D and N) were studied as coarse aggregate in combination with three natural sands of different reactivity (Table 1). Aggregate potential for reactivity is indicated by 14-day expansion values over 0.2%. Petrographic

analysis revealed minerals present in greywacke aggregate: mainly quartz (various forms including micro and cryptocrystalline quartz), plagioclase, and K-feldspar. Reactive silica was present in fine aggregate as micro and cryptocrystalline quartz, and chert [19]. The greywackes had similar oxide compositions (Table 2), however, the N greywacke had a slightly higher SiO_2 and Al_2O_3 content than the D greywacke. Natural fossil sand is quarried from sedimentary deposits; it consists of fine grains of quartz and carbonate minerals that also may contain microscopic fossil fragments.

Portland cement CEM I 52.5 R with an alkali content of 0.88% Na_2O_{eq} was used for reference concrete mixtures. Two types of ASR-inhibiting materials were tested—metakaolin and ground granulated blast furnace slag. Metakaolin is a commercial pozzolanic additive type II according to the standard EN 206 [20], with a density of 2.69 g/cm^3 and a specific surface area of 20,000 cm^2/g. Metakaolin was used as a partial mass replacement for Portland cement. Ground granulated blast furnace slag was used as a constituent of factory-produced blended cements CEM II/B-S 42.5 R and CEM IIIA 42.5 N (Ożarów Cement, Poland), with slag contents of about 35% and 52%, respectively. The chemical composition of the cement is given in [21].

Table 1. Characteristics of coarse and fine aggregates.

ID	Description		Density [g/cm^3]	Expansion * [%]	
				At 14 Days	At 28 Days
D	coarse	Crushed greywacke	2.71	0.31	0.52
N		Crushed greywacke	2.73	0.26	0.40
B	fine	Natural fossil sand	2.65	0.09	0.23
W		Natural river sand	2.66	0.30	0.46
T		Natural fossil sand	2.65	0.36	0.57

* according to accelerated mortar bar test ASTM C1260 [22].

Table 2. Chemical composition of aggregates determined by XRF *.

Constituent	Content [%]				
	Greywacke (D)	Greywacke (N)	Sand (B)	Sand (W)	Sand (T)
SiO_2	58.27	63.22	87.15	93.52	89.98
TiO_2	0.74	0.659	0.075	0.035	0.1
Al_2O_3	14.51	15.11	2.61	1.5	2.98
Fe_2O_3	5.79	5	0.52	0.23	0.49
MnO	0.116	0.062	0.015	0.009	0.027
MgO	2.24	1.97	0.19	0.02	0.30
CaO	2	1.32	2.48	0.17	1.28
Na_2O	2.08	2.93	0.49	0.29	0.57
K_2O	2.78	3.01	0.95	0.54	1
P_2O_5	0.189	0.152	0.06	0.017	0.028
SO_3	0.13	<0.01	<0.01	<0.01	<0.01
Cl	0.014	0.016	0.001	0.007	<0.001
F	<0.01	<0.01	<0.01	0.04	<0.01
LOI	6.9	1.9	2.2	<0.5	1.7
total	95.64	95.21	96.71	96.66	98.41

* X-ray spectrometer with wavelength dispersion—Philips WD-XRF PW 2400 (Philips N.V., Eindhoven, The Netherlands). Notes: the main constituent > 1.0%; the secondary constituent <1.0–0.01%>.

The combinations of cement, coarse and fine aggregates, and supplementary cementitious material dosage are presented in Table 3. The concrete mix design followed the

standard specification of AASHTO T380 [23]: the cement content of 420 kg/m^3, water-to-cement ratio of 0.45, maximum aggregate size of 12.5 mm, and NaOH was used for alkali boosting up to Na_2O_{eq} content of 1.25%. The specification was slightly modified to include aggregate blends of different potential reactivity.

Table 3. Key constituents of concrete mixtures.

Mix ID	Cement	Coarse Aggregate	Fine Aggregate	Mitigating Compound	Dosage
DB0	CEM I 52.5R	Greywacke (D)	Non-reactive sand (B)	None	-
DBM7				Metakaolin	7.5%
DBM15				Metakaolin	15%
DW0	CEM I 52.5R	Greywacke (D)	Reactive sand (W)	None	-
DWS35	CEM II/B-S 42.5R			GGBS (as cement constituent)	ca. 35%
DWS52	CEM III/A 42.5N			GGBS (as cement constituent)	ca. 52%
DWM7	CEM I 52.5R			Metakaolin	7.5%
DWM15	CEM I 52.5R			Metakaolin	15%
DT0	CEM I 52.5R	Greywacke (D)	Reactive sand (T)	None	-
DTS35	CEM II/B-S 42.5R			GGBS (as cement constituent)	ca. 35%
DTM7	CEM I 52.5R			Metakaolin	7.5%
DTM15	CEM I 52.5R			Metakaolin	15%
NB0	CEM I 52.5R	Greywacke (N)	Non-reactive sand (B)	None	-
NBM7				Metakaolin	7.5%
NBM15				Metakaolin	15%
NBM20				Metakaolin	20%

2.2. Methods

The aggregate mixture reactivity and the effectiveness of ASR mitigation measures were evaluated by monitoring the expansion of concrete samples over time according to [23]. For each concrete mixture three standard prismatic samples (50 mm × 50 mm × 285 mm with steel studs) were cast, cured, and immersed in a 1 molar NaOH solution at 60 °C for 84 days, while similar companion samples were stored in water at standard laboratory temperature (reference specimens). The standard expansion evaluation period is 56 days but it has been suggested that extended storage is appropriate for evaluation of mitigation measures. The photo illustration of the main elements of the laboratory investigation on concrete specimens is shown in Figure 1. Periodically, expansion measurements were taken, and the resonant frequency of flexural vibrations was measured using a GrindoSonic MK5 device (GrindoSonic BV, Leuven, Belgium) to determine the resonant elastic modulus of concrete as per ASTM C215 [24]. After the immersion period, the compressive strength of the concrete was evaluated using a modified standard procedure on 50 mm cubic specimens cut from the concrete prisms. Small labs were cut from the cross-section of prismatic samples for microstructural observations using a scanning electron microscope with an EDS detector. The cut specimens, 30 mm × 40 mm × 10 mm in size, were protected with epoxy resin, polished, and then sputter coated with carbon. Microstructural observations were performed using a JEOL JSM-6460LV (Jeol Ltd., Tokyo, Japan) with the following

operating conditions: acceleration voltage of 20 kV, an aperture of 120 µm, and a working distance of 10 mm.

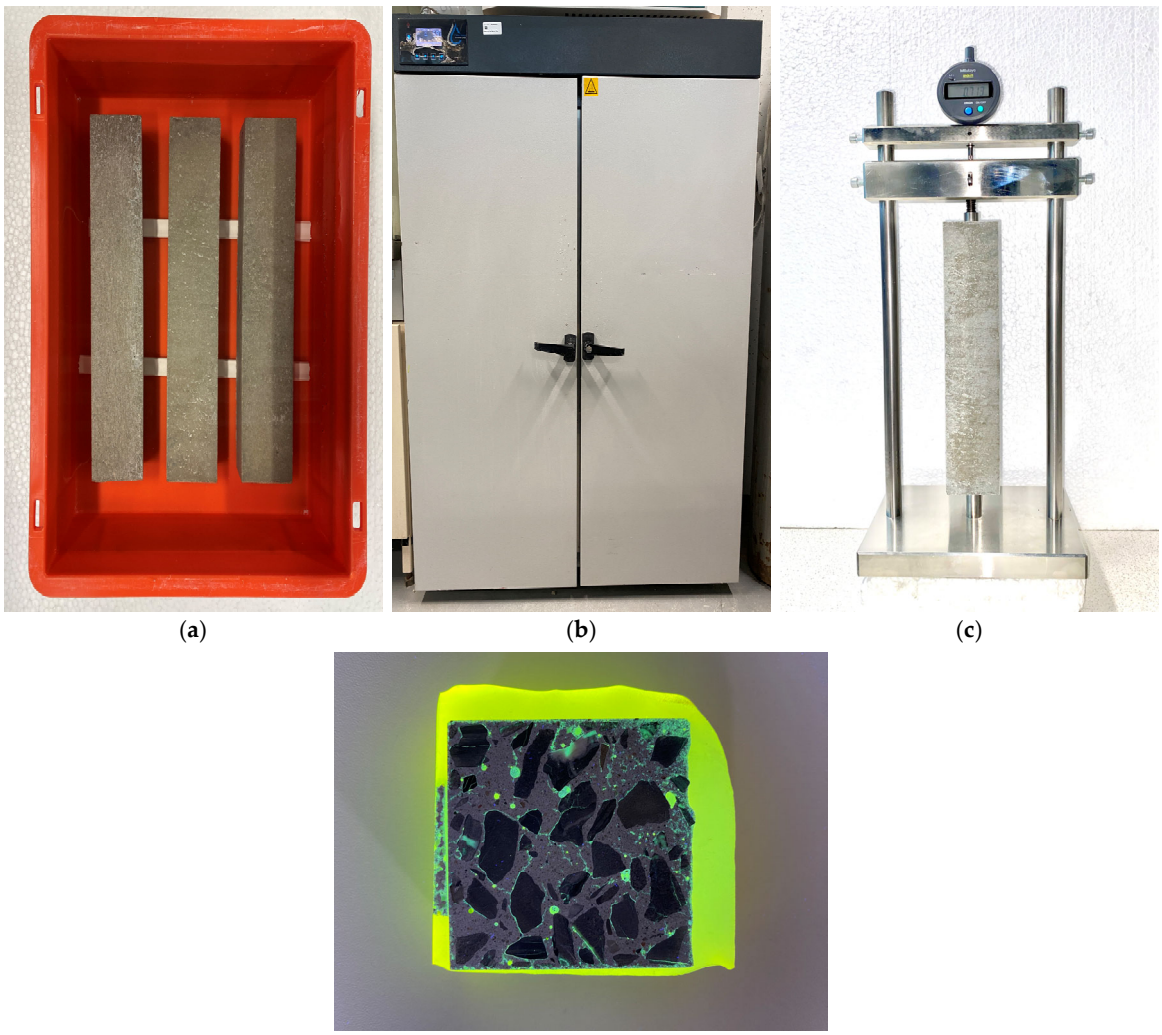

Figure 1. Illustration of the main elements of the laboratory investigation on concrete specimens: (**a**) specimens in NaOH solution, (**b**) the 60 °C storage cabinet, (**c**) measurement of elongation, and (**d**) cracks seen in the cross section of prismatic specimen.

Following the resonance modulus testing, selected prismatic specimens were used for microscopic crack detection. After drying at 30 °C for 72 h they were vacuum-impregnated with epoxy resin containing a fluorescent dye. Perpendicular slices, each 30 mm thick, were extracted from the prismatic specimens and polished to achieve a smooth, even surface. After drying, they were re-impregnated and polished once more to eliminate any surplus fluorescent resin, adhering to the method outlined in [25] (Figure 1d). The width of cracks was examined under UV light using a digital microscope.

3. Results

3.1. Expansion

In Figure 2, the expansion development over time is shown for the concrete mixtures. The standard deviation of the expansion data was low, ranging from 0.001 to 0.011%. For a clear readability the expansion curves are presented in four groups: (a) mixtures without supplementary cementitious materials, (b) with low dose of metakaolin (7.5%), (c) with high dose of metakaolin (15–20%), and (d) with slag-blended cements. Following the AASHTO

T380 standard criteria (shown by the dashed lines in Figure 2), the tested aggregate mixtures with greywacke showed moderate to high reactivity in MCPT tests. Despite an initial low expansion (up to 14 days), the highest expansion was observed in concrete samples with greywacke N and non-reactive sand B (0.22%), which was twice as high as samples with greywacke D and the same sand. The presence of reactive sand in the mixture with moderately reactive greywacke increased the expansion of concrete samples—with a stronger increase observed for higher potential reactivity of sand according to Table 1 data. A lower dose of metakaolin (Figure 2b) and the use of CEM II/B-S (Figure 2d) had a similar effect on the expansion over time. They significantly changed the slope of the curves compared to the reference concretes (Figure 2a), but not enough to meet the AASHTO criteria (<0.020% at 56 days). The addition of 15–20% metakaolin (Figure 2c) and CEM III/A (Figure 2d) most effectively lowered the rate of expansion over time, almost flattening the expansion curves, and met the criteria for efficiency of ASR mitigation measures.

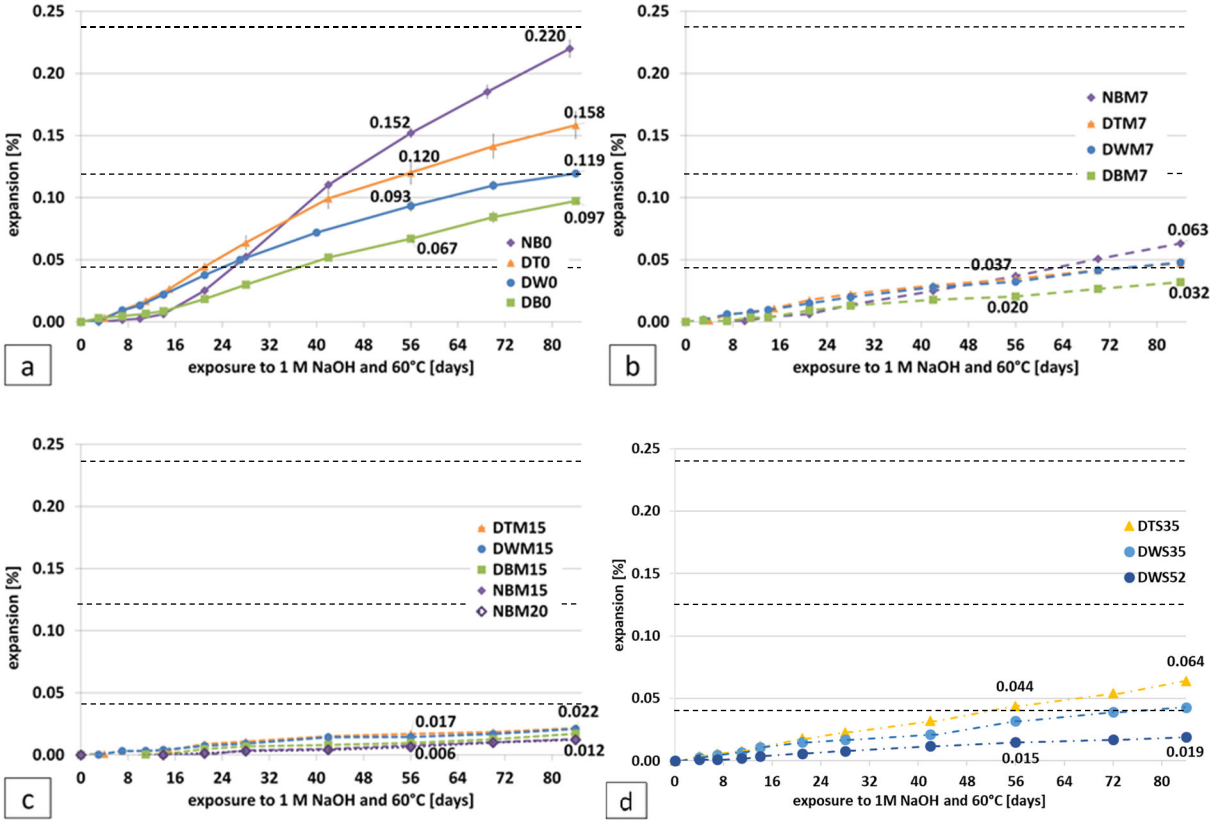

Figure 2. Expansion of concrete with greywacke aggregate (D, N) and different fine aggregate (B, W, T) exposed to 1 M NaOH solution at 60 °C (**a**) without supplementary cementitious materials, (**b**) with low dose of metakaolin (7.5%), (**c**) with high dose of metakaolin (15–20%), (**d**) with slag-blended cements (dashed lines—AASHTO T380 standard criteria: ≥0.04% moderately reactive, ≥0.12% highly reactive; the mixture notation according to Table 3).

Expansion results at 56 and 84 days of exposure, and the relative reduction in expansion in comparison to reference mixtures, are summarized in Table 4. A strong reduction in expansion was observed with metakaolin addition, proportional to its content (Figure 3). For greywacke N, this relationship is better reflected by an exponential rather than a linear trend. A 7.5% content of metakaolin resulted in a 65–75% reduction in expansion; the mitigation of expansion was more efficient for higher reactivity of both coarse and fine aggregate. The expansion mitigation effectiveness of metakaolin over the extended test period was similar or lower than after 56 days. A sufficient amount of metakaolin to

provide a safe reduction in expansion (<0.020%) was 15%, which provided an 85–95% reduction in initial expansion. Increasing the dosage to 20% slightly reduced the expansion, but not significantly (by about 1%).

Table 4. Expansion of samples with greywacke aggregate and supplementary cementitious materials for ASR mitigation.

Mix ID	Average Expansion [%]			
	56 Days	Rel. Reduction [%]	84 Days	Rel. Reduction [%]
DB0	0.067	-	0.097	-
DBM7	0.020	70.1	0.032	67.0
DBM15	0.010	85.1	0.017	82.5
DW0	0.093	-	0.119	-
DWS35	0.032	65.6	0.043	63.9
DWS52	0.015	83.9	0.019	84.0
DWM7	0.032	65.6	0.048	59.7
DWM15	0.014	84.9	0.021	82.4
DT0	0.120	-	0.158	-
DTS35	0.044	63.3	0.064	59.4
DTM7	0.035	70.8	0.047	70.3
DTM15	0.017	85.8	0.022	86.1
NB0	0.152	-	0.220	-
NBM7	0.037	75.7	0.063	71.4
NBM15	0.008	94.7	0.013	94.1
NBM20	0.006	96.1	0.012	94.5

Note: the expansion limit for prevention: 0.02% at 56 days of exposure (in yellow); 0.025% at 84 days of exposure (in blue).

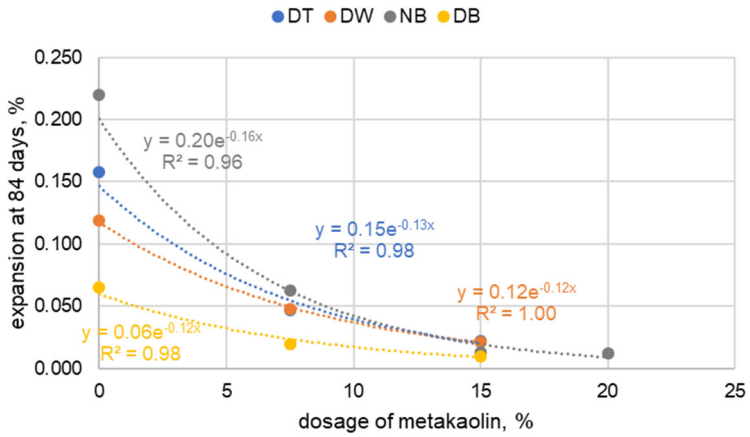

Figure 3. Relationship between 84-day expansion of concrete specimens and the content of metakaolin.

The use of slag-blended cements resulted in a reduction in expansion at a similar level to metakaolin addition: the effect of CEM II/B-S corresponded to a dosage of 7.5% metakaolin, while CEM III/A effectiveness was similar to about 15% metakaolin. The effectiveness of the slag-blended cement also depended on the reactivity of the aggregate mixture—replacing the W sand with the more reactive T sand slightly reduced its ability to mitigate the expansion.

3.2. Elastic Modulus and Compressive Strength

The effects of specimen storage conditions on selected mechanical properties of concrete are summarized in Table 5. For reference specimens (DB0, DW0, DT0, NB0), a relative decrease in compressive strength due to the exposure to NaOH solution at 60 °C ranged

from 3 to 21% in comparison to specimens stored in water at 20 °C. The associated reduction in the resonant elastic modulus ranged from 15 to 24%, showing a stronger reduction when using reactive sand W or T.

Table 5. Compressive strength and modulus of elasticity of concrete specimens stored for 84 days in water or in 1 molar NaOH solution.

Mix ID	Compressive Strength [MPa] *			Resonance Elastic Modulus [GPa] **		
	NaOH 60 °C	H_2O 20 °C	Rel. Loss [%]	NaOH 60 °C	H_2O 20 °C	Rel. Loss [%]
DB0	57.2 ± 2.9	59.0 ± 1.5	3.1	41.5	49.0	15.3
DBM7	57.0 ± 1.9	61.5 ± 1.3	7.4	46.7	48.1	2.9
DBM15	56.5 ± 1.5	59.8 ± 0.8	5.4	48.4	44.9	−7.7
DW0	64.3 ± 3.5	73.1 ± 4.8	12.0	37.6	49.5	24.0
DWS35	64.7 ± 3.6	63.3 ± 1.7	−2.2	44.5	47.4	6.1
DWS52	58.9 ± 2.1	54.6 ± 2.6	−7.9	44.2	48.2	8.3
DWM7	73.2 ± 2.8	69.9 ± 5.4	−4.7	43.2	46.5	7.1
DWM15	67.8 ± 3.4	72.6 ± 4.7	6.6	42.8	47.1	9.1
DT0	64.2 ± 2.1	73.9 ± 1.9	13.2	38.9	49.9	22.0
DTS35	65.1 ± 2.4	65.8 ± 0.9	1.0	47.1	49.5	4.8
DTM7	72.5 ± 2.8	72.5 ± 3.9	0.0	44.3	47.3	6.3
DTM15	67.0 ± 3.1	72.3 ± 3.5	7.3	43.8	48.5	9.7
NB0	63.4 ± 2.5	80.2 ± 3.5	20.9	N/A ***	N/A ***	-
NBM7	71.5 ± 1.8	74.0 ± 1.6	3.4	44.0	54.0	18.5
NBM15	64.1 ± 1.8	65.6 ± 3.4	2.2	45.0	48.4	7.0
NBM20	61.7 ± 2.7	66.7 ± 1.8	7.5	47.4	47.9	1.0

* average value ± standard deviation, ** coefficient of variation from 0.5% to 6.7%, *** missing results due to equipment malfunction.

Most concrete samples containing supplementary cementitious materials stored in NaOH solution exhibited slightly lower compressive strength than specimens stored in water, with a reduction up to 8%. Exceptionally, slag-blended cements induced a reverse trend exhibiting the increase in compressive strength by 2 to 8%, possibly due to the pozzolanic reaction enhanced by the increased temperature. Metakaolin addition impeded the decrease in the elastic modulus of concrete exposed to ASR-promoting storage conditions, limiting it to 10%. This was effective for greywacke blends with both non-reactive and reactive fine aggregates. In the case of slag-blended cement, the degradation of compressive strength and elastic modulus due to ASR was clearly mitigated. The decrease in elastic modulus as a result of immersion in NaOH solution at 60 °C did not exceed 8%, while the compressive strength remained stable, exhibiting changes of only a few percent that were indistinguishable from data scatter.

3.3. Reaction Products in Concrete Specimens

Alkali–silica reaction products in Portland cement concrete specimens with no mineral additions were primarily found in cracks within the coarse aggregate. Both amorphous and crystalline products were identified, but crystalline ones were predominant (Figure 4). No presence of ASR products was detected in fine aggregate grains in concrete containing non-reactive sand, contrary to mixtures containing reactive sands (W, T) which showed grains that reacted to form ASR gel (Figures 5 and 6).

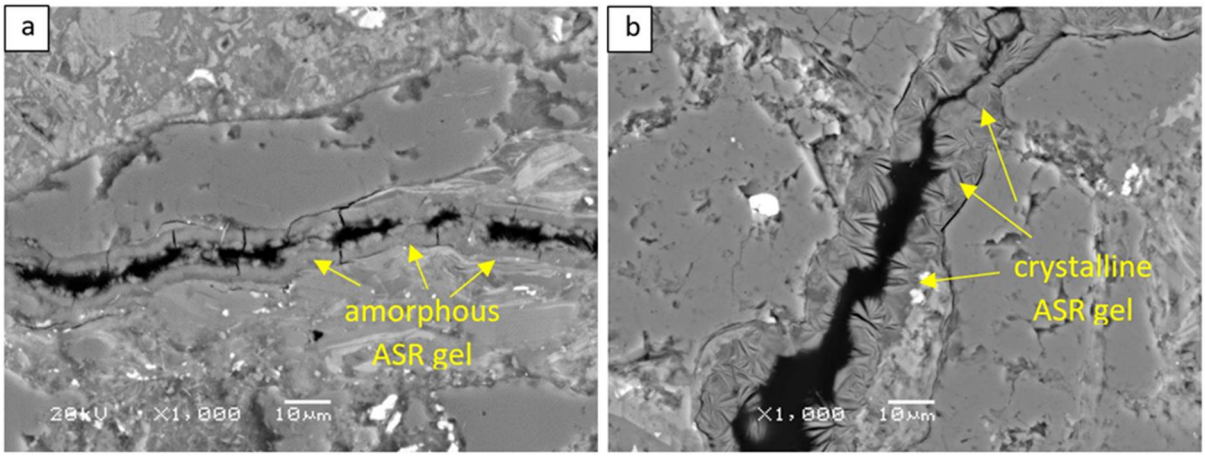

Figure 4. Microstructural features of Portland cement concrete (DB0) with greywacke aggregate (D) and nonreactive sand (B)—crack in greywacke grain filled with alkali–silica reaction product: (**a**) amorphous, (**b**) crystalline.

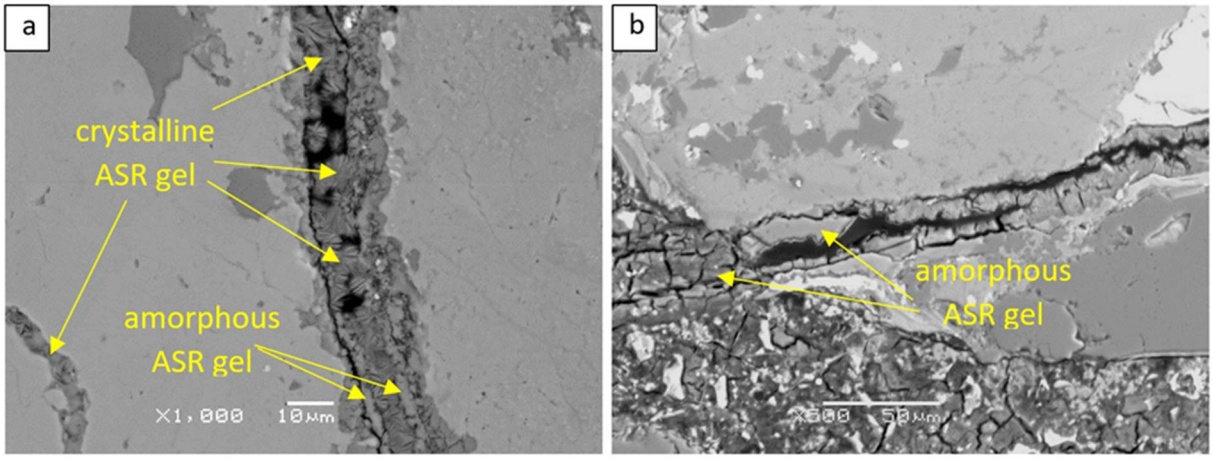

Figure 5. Amorphous and crystalline alkali–silica reaction products (**a**,**b**) filling cracks in greywacke grain in (DW0) Portland cement concrete specimen.

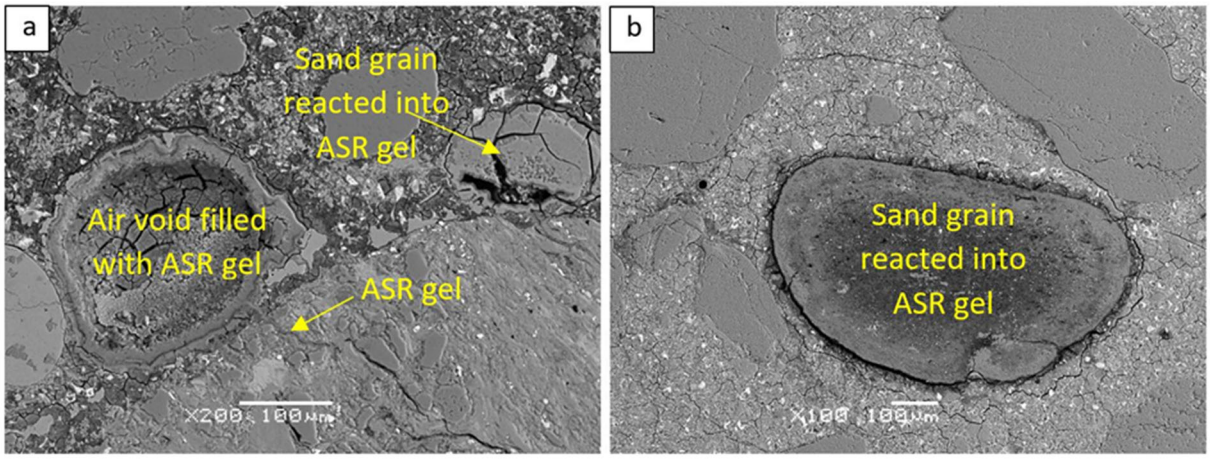

Figure 6. Sand grains reacted into ASR gel, air void filled with ASR product in Portland cement concrete specimens with reactive fine aggregate: (**a**) mix DT0 and (**b**) mix DW0.

The addition of metakaolin to concrete mixtures mitigated the negative effects of greywacke reactivity (Figure 7). Fewer cracks were observed in the greywacke aggregate,

and only some of them were filled with reaction products, while others remained empty. No grains of sand that reacted to form ASR gel were found. However, the reaction was not entirely stopped, and traces were observed in both the coarse aggregate and cement matrix. Similarly, the use of blast furnace slag in blended cements had a strong effect on reducing the ASR development (Figure 8). The majority of cracks in the aggregate were empty, and the number and width of cracks in the cement matrix were significantly reduced.

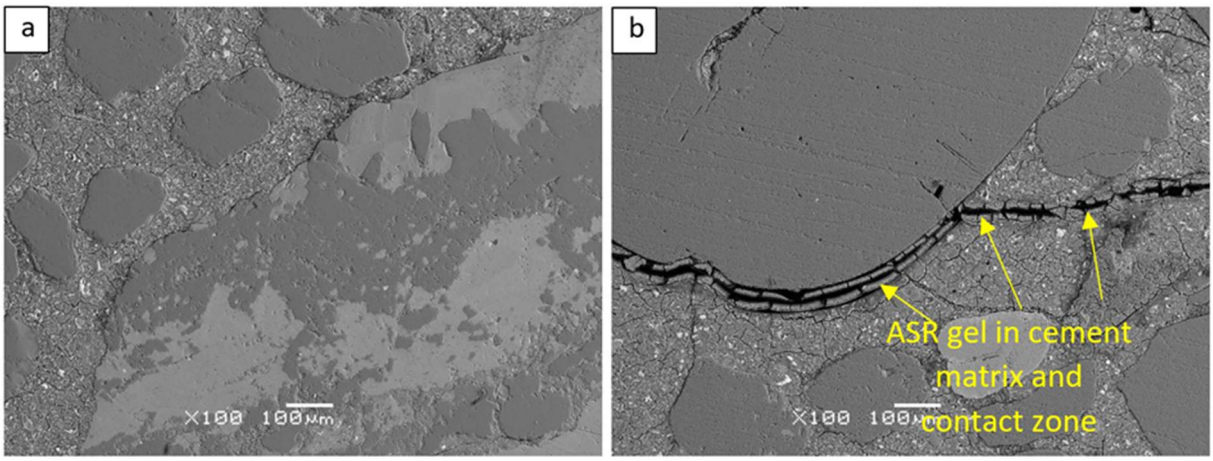

Figure 7. Microstructural features of concrete containing metakaolin (DTM15) with greywacke aggregate (D) and reactive sand (T)—greywacke and sand grains without signs of ASR (**a**), and ASR product in cement matrix and aggregate contact zone (**b**).

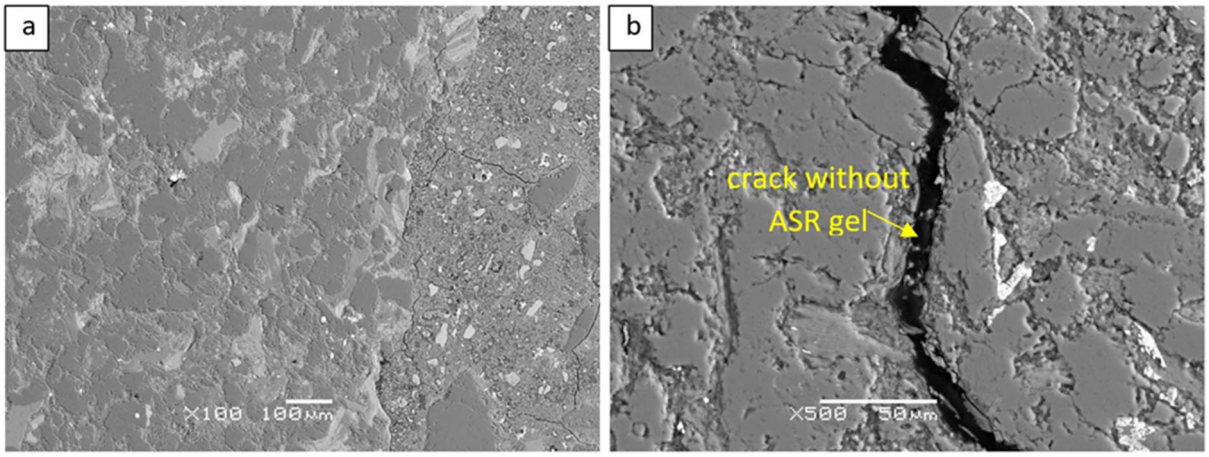

Figure 8. Microstructural features of slag-blended cement concrete (DWS35) with greywacke aggregate (D) and reactive sand (W)—greywacke and sand grains without signs of ASR (**a**), and crack in greywacke grain without alkali-silica products (**b**).

The composition of the reaction products in greywacke aggregate was slightly dependent on their morphology. Crystalline products were characterized by a slightly higher alkali content, with a Na + K/Si ratio of 0.25 (±0.03), compared to amorphous products, which had a Na + K/Si ratio of 0.21 (±0.03). The calcium content in ASR products within aggregate cracks was similar regardless of the product's morphology, with a Ca/Si ratio of 0.31 (±0.03). The reaction products in the cement matrix and air voids had higher calcium content and lower alkali content compared to the products in the aggregate with a Na + K/Si ratio of 0.18 (±0.04) and a Ca/Si ratio of 0.42 (±0.03).

Microscopic examination of cracks in the cross section revealed the presence of short cracks with the maximum width from 0.1 to 0.2 mm in the specimens manufactured with Portland cement without supplementary cementitious materials. The cracks primarily

appeared around aggregate grains and within the cement matrix. Only tiny cracks, less than 0.1 mm in width, were detected in the specimens containing metakaolin or granulated blast furnace slag. It is likely that certain cracks previously filled with ASR products were not penetrated by the epoxy resin during sample preparation. Considering the crack width limits associated with the degree of ASR intensity [26], the effectiveness of applied supplementary cementitious materials can be confirmed.

4. Discussion

The current investigation using the AASHTO T380 test method revealed a moderate reactivity potential in greywacke aggregate that is in accordance with previous evaluations using the accelerated mortar bar tests [27]. Although some differences were expected, following the general knowledge of the temperature influence [28] and the inadequacy of the accelerated mortar bar test for greywacke aggregate [29] (at least for New Zealand deposits), that was not the case.

The moderate reactivity potential seems to corroborate with the presence of moderately reactive minerals, like micro- and crypto-crystalline quartz [12]. SEM EDS examination of concrete provided evidence for alkali–silica reaction as the cause of the observed expansive behavior, detecting both crystalline and amorphous reaction products of typical composition [30]. The associated loss in elastic properties and strength of concrete (Table 5) was proportional to the observed expansion but it did not exceed 24% for reference concrete mixes, substantially lower than the findings by Thomas et al. for greywacke from Wales [15].

There is an implication that some greywackes may exhibit a mechanism of intrinsic ASR inhibition related to the occurrence and release of aluminum by clay minerals [31], potentially explaining the unique non-reactivity of greywackes from New Zealand. The formation of zeolites or zeolite precursors (alkali-silicate phase) in concrete was observed at high temperature (80 °C) and high alkali concentration (0.5–1 mol/L NaOH or KOH). An inverse relationship was found between the rate of silica release by the aggregate and the amount of zeolite formed at the same temperature. The formation of alkali aluminosilicate and zeolite reduces the concentration of so-called "free" silica available for ASR, thereby inhibiting ASR. On the other hand, Shi and Lothenbach [32] point out that the formation of alkali aluminosilicate or zeolite at lower temperatures is too slow (decades) to be important in inhibiting ASR formation in concrete structures. Even if this mechanism does not occur naturally, it may contribute to the perturbation of the 80 °C accelerated test results. The slightly higher content of both Al_2O_3 and SiO_2 in the N aggregate, relative to the D aggregate, may indicate that the expansion in the 80 °C accelerated test of the potentially more reactive N aggregate (more silica) was inhibited by the increased clay mineral content.

The effects of metakaolin and granulated blast furnace slag on the expansion of concrete with greywacke aggregate have been previously studied, but to a limited extent. The current findings extend the recognition of these supplementary cementitious materials for greywacke blends with moderately reactive fine aggregate. The effectiveness of such mitigation measures is demonstrated by the radically changed kinetics of concrete expansion—down below 0.02% at 56 days of exposure. This effectiveness is confirmed by a minor reduction in elastic properties (5 to 8%), and pretty stable compressive strength as well as the lack of alkali–silica reaction products in the concrete. These results are considered conservative as they were obtained in a 1 molar NaOH solution. MCPT test data are considered to be well correlated with natural exposure blocks data [33,34], much better than the accelerated mortar bar test and even better than concrete prism test data. A good correlation with natural exposure data is a key observation to evaluate the significance of laboratory test results [35]. A recent evaluation of such correlations for several laboratory

test methods [34] regarding ASR mitigation effectiveness resulted in a proposed change of criteria for MCPT test results: an expansion limit of 0.025% to be applied to 84 days of exposure data. As shown in Table 4, such a criterion modification does not change the evaluation of the preventive options: the results for metakaolin and slag-blended cement still confirm the effectiveness of ASR mitigation in concrete containing moderately reactive greywacke and moderately reactive quartz sand.

It is important to note that the actual environmental exposure of concrete in road pavements, characterized by changes in temperature and humidity, as well as road traffic loads, may be far more complex than the exposure conditions of specimens tested according to the MCPT method. The significance of MCPT has been established in respect to the previously mentioned natural exposure blocks performance [33,34] but no traffic loads were considered. However, the standard soak solution is highly alkaline so the possible effects of external alkali supply might be covered with a sufficient margin of confidence.

The significance of current findings for pavement concrete mix design is limited to only one aspect of the desired concrete durability, while in wet-freeze climate zones its frost-resistance and scaling resistance will also be very important. A possible interaction of ASR and freeze-thaw induced cracking or deicing salt exposure may lead to premature concrete damage, as shown in laboratory studies [36–38]. Such interaction of aggressive factors leading to the premature damage of concrete highway pavement was also revealed in full-scale diagnostic studies [26,39]. The mechanisms of such possible interaction are not well understood; therefore, the topic requires further studies.

5. Conclusions

The following conclusions can be drawn.

1. A moderate alkaline reactivity of locally sourced greywacke aggregate was established using the MCPT method. The expansion, due to alkali–silica reaction, was increased by a factor 1.7–2.4 when greywacke coarse aggregate was blended with natural sand of moderate reactivity.
2. Alkali–silica reaction products in Portland cement concrete, both crystalline and amorphous, were detected in the cracks of greywacke grains, around greywacke grains, and in the cement matrix. In the blends with reactive fine aggregate, the alkali–silica reaction products filled the space previously occupied by reactive sand grains. The composition of reaction products in greywacke grains was characterized by the Ca/Si ratio of about 0.31 ($\pm$ 0.03), the (Na + K)/Si ratio of about 0.25 ($\pm$ 0.03), and 0.21 ($\pm$ 0.03) for crystalline and amorphous products, respectively.
3. Metakaolin used for partial replacement of Portland cement and ground-granulated blast furnace slag used as a constituent of blended cements were found effective in mitigating the expansion of concrete containing greywacke aggregate and moderately reactive quartz sand. The required level of ASR mitigation is obtained for the replacement of 15% of Portland cement by metakaolin or the use of CEM III/A cement containing about 52% of slag.
4. The expansion of concrete containing greywacke aggregate was associated with a trend of the reduction of the resonant elastic modulus by 15 to 24%. The use of metakaolin or slag-blended cements resulted in stabilization of the compressive strength of concrete and limiting the deterioration of elastic modulus below 10%.

Author Contributions: Conceptualization, K.D. and M.A.G.; methodology, K.D. and M.A.G.; validation, K.D. and M.A.G.; formal analysis, K.D. and A.B.; investigation, K.D., A.B., and D.N.; data curation, K.D.; writing—original draft preparation, K.D.; writing—review and editing, A.B., D.N.,

and M.A.G.; visualization, K.D. and A.B.; supervision, M.A.G.; funding acquisition, K.D. and M.A.G. All authors have read and agreed to the published version of the manuscript.

Funding: This research was funded by the Polish National Science Centre as part of Preludium Project no. 2023/49/N/ST8/02157.

Institutional Review Board Statement: Not applicable.

Informed Consent Statement: Not applicable.

Data Availability Statement: The raw data supporting the conclusions of this article will be made available by the authors on request.

Conflicts of Interest: The authors declare no conflicts of interest.

Abbreviations

The following abbreviations are used in this manuscript:

ASR	Alkali–silica reaction
MCPT	Miniature concrete prism test
D	Coarse crushed greywacke
N	Coarse crushed greywacke
B	Natural fossil sand
W	Natural river sand
T	Natural fossil sand
XYZA	Mix ID, where X—type of coarse aggregate, Y—type of fine aggregate, Z—mitigating compound, and A—dosage of mitigating compound
XRF	X-ray Fluorescence

References

1. Rens, L. European Guide for Design of "Jointed Plain Concrete Pavements", Concrete Paving Association, Brussels. 2020. Available online: https://www.eupave.eu/wp-content/uploads/EUPAVE-Guide-for-the-design-of-jointed-plain-concrete-pavements-April-2020.pdf (accessed on 26 May 2025).
2. Glinicki, M.A. Concrete durability evaluation in new built pavement sections of expressways in Poland. *Cement Wapno Beton* **2023**, *28*, 105–119. [CrossRef]
3. Rudnicki, T. The impact of the aggregate used on the possibility of reducing the carbon footprint in pavement concrete. *Sustainability* **2022**, *14*, 16478. [CrossRef]
4. Van Dam, T.; Taylor, P.; Fick, G.; VanGeem, M.; Lorenz, E. *Sustainable Concrete Pavements: A Manual of Practice*; Institute for Transportation, Iowa State University: Ames, IA, USA, 2012.
5. Rudnicki, T.; Stałowski, P. Performance research of cement concrete pavements with a lower carbon footprint. *Materials* **2024**, *17*, 3162. [CrossRef]
6. Wang, F.; Xie, J.; Wu, S.; Li, J.; Barbieri, D.M.; Zhang, L. Life cycle energy consumption by roads and associated interpretative analysis of sustainable policies. *Renew. Sustain. Energy Rev.* **2021**, *141*, 110823. [CrossRef]
7. Smith, S.H.; Durham, S.A. A cradle to gate LCA framework for emissions and energy reduction in concrete pavement mixture design. *Int. J. Sustain. Built Environ.* **2016**, *5*, 23–33. [CrossRef]
8. *EN 1097-8*; Tests for Mechanical and Physical Properties of Aggregates–Part 8: Determination of the Polished Stone Value. CEN: Brussels, Belgium, 2020.
9. *EN 1097-1*; Tests for Mechanical and Physical Properties of Aggregates–Part 1: Determination of the Resistance to Wear (Micro-Deval). CEN: Brussels, Belgium, 2011.
10. *EN 1097-2*; Tests for Mechanical and Physical Properties of Aggregates–Part 2: Methods for the Determination of Resistance to Fragmentation. CEN: Brussels, Belgium, 2020.
11. General Directorate for National Roads and Highways (GDDKiA). Conditions for the Execution and Acceptance of Construction Works D- 05.03.04 v02. Cement Concrete Pavements. Available online: https://www.gov.pl/web/gddkia/nawierzchnie (accessed on 26 May 2025). (In Polish)
12. Fernandes, I.; Ribeiro, A.M.; Broekmans, M.; Sims, I. *Petrographic Atlas: Characterisation of Aggregates Regarding Potential Reactivity to Alkalis. RILEM TC 219-ACS Recommended Guidance AAR-1.2, for Use with the RILEM AAR-1.1 Petrographic Examination Method*; Springer: Dordrecht, The Netherlands, 2016.

13. Shayan, A.; Quick, G.W.; Lancucki, C.J.; Way, S.J. Investigation of some greywacke aggregates for alkali silica reactivity. In Proceedings of the 9th International Conference on Alkali-Aggregate Reaction in Concrete, London, UK, 27–32 July 1992.
14. Moffatt, E.G.; Thomas, M.D.A.; Hayman, S.; Fournier, B.; Ideker, J.; Fletcher, J. Remediation Strategies Intended for the Reconstruction of the ASR-Induced Mactaquac Dam. In Proceedings of the 15th International Conference on Alkali-Aggregate Reaction in Concrete, Sao Paulo, Brazil, 3–7 July 2016.
15. Thomas, M.; Dunster, A.; Nixon, P.; Blackwell, B. Effect of fly ash on the expansion of concrete due to alkali-silica reaction—Exposure site studies. *Cem. Concr. Compos.* **2011**, *33*, 359–367. [CrossRef]
16. Tremblay, C.; Bérubé, M.A.; Fournier, B.; Thomas, M.D.; Folliard, K.J. Experimental investigation of the mechanisms by which $LiNO_3$ is effective against ASR. In Proceedings of the 13th International Conference on Alkali-Aggregate Reaction in Concrete, Trondheim, Norway, 16–20 June 2008.
17. Ramlmochan, T.; Thomas, M.; Gruber, K.A. The effect of metakaolin on alkali–silica reaction in concrete. *Cem. Concr. Res.* **2000**, *30*, 339–344. [CrossRef]
18. Richardson, M. Minimising the risk of deleterious alkali-silica reaction in Irish concrete practice. *Constr. Build. Mater.* **2005**, *19*, 654–660. [CrossRef]
19. Jóźwiak-Niedźwiedzka, D.; Antolik, A.; Dziedzic, K.; Gméling, K.; Bogusz, K. Laboratory investigations on fine aggregates used for concrete pavements due to the risk of ASR. *Road Mater. Pavement Des.* **2021**, *22*, 2883–2895. [CrossRef]
20. *EN 206*; Concrete–Specification, Performance, Production and Conformity. CEN: Brussels, Belgium, 2013.
21. Dziedzic, K.; Glinicki, M.A. Risk assessment of reactive local sand use in aggregate mixtures for structural concrete. *Constr. Build. Mater.* **2023**, *408*, 133826. [CrossRef]
22. *ASTM C1260*; Standard Test Method for Potential Alkali Reactivity of Aggregates (Mortar-Bar Method). ASTM International: West Conshohocken, PA, USA, 2023.
23. *AASHTO T 380-2019*; Standard Method of Test for Potential Alkali Reactivity of Aggregates and Effectiveness of ASR Mitigation Measures (Miniature Concrete Prism Test, MCPT). American Association of State Highway and Transportation Officials: Washington, DC, USA, 2019.
24. *ASTM C215-14*; Standard Test Method for Fundamental Transverse, Longitudinal, and Torsional Resonant Frequencies of Concrete Specimens. ASTM International: West Conshohocken, PA, USA, 2014.
25. Glinicki, M.A.; Litorowicz, A. Crack system evaluation in concrete elements at mesoscale. *Bull. Pol. Acad. Sci.-Tech. Sci.* **2006**, *54*, 371–379.
26. Borchers, I. Leistungsbasiertes Konzept Für Einen Ausreichenden AKR-Widerstand Von Beton (Performance-Based Concept for Sufficient ASR Resistance of Concrete). Ph.D. Thesis, Technischen Universität Clausthal, Clausthal-Zellerfeld, Germany, 2023.
27. Glinicki, M.A.; Jóźwiak-Niedźwiedzka, D.; Antolik, A.; Dziedzic, K.; Gibas, K. Susceptibility of selected aggregates from sedimentary rocks to alkali-aggregate reaction. *Roads Bridges Drog. I Mosty* **2019**, *18*, 5–24. [CrossRef]
28. Kawabata, Y.; Dunant, C.; Nakamura, S.; Yamada, K.; Kawakami, T. Effects of temperature on expansion of concrete due to the alkali-silica reaction: A simplified numerical approach. *Mater. De Construcción* **2022**, *72*, e282. [CrossRef]
29. Freitag, S.A.; St John, D.A.; Goguel, R. ASTM C1260 and the alkali reactivity of New Zealand greywackes. In Proceedings of the 11th International Conference on Alkali-Aggregate Reaction in Concrete, Quebec City, QC, Canada, 11–16 June 2000.
30. Leemann, A.; Shi, Z.; Lindgård, J. Characterization of amorphous and crystalline ASR products formed in concrete aggregates. *Cem. Concr. Res.* **2000**, *137*, 106190. [CrossRef]
31. Hünger, K.J. The contribution of quartz and the role of aluminum for understanding the AAR with greywacke. *Cem. Concr. Res.* **2007**, *37*, 1193–1205. [CrossRef]
32. Shi, Z.; Lothenbach, B. Role of Aluminum and Lithium in Mitigating Alkali-Silica Reaction–A Review. *Front. Mater.* **2022**, *8*, 796396. [CrossRef]
33. Konduru, H.; Rangaraju, P.R.; Amer, O. Reliability of Miniature Concrete Prism Test in Assessing Alkali-Silica Reactivity of Moderately Reactive Aggregates. *Transp. Res. Rec.* **2020**, *2674*, 23–29. [CrossRef]
34. National Academies of Sciences, Engineering, and Medicine. *Alkali-Silica Reactivity Potential and Mitigation: Test Methods and State of Practice*; The National Academies Press: Washington, DC, USA, 2023. [CrossRef]
35. Leemann, A.; Merz, C. Long-term efficiency of silica fume and fly ash to suppress ASR in field structures. *Mater. De Construcción* **2022**, *72*, e285. [CrossRef]
36. Deschenes, R.A.; Giannini, E.R.; Drimalas, T.; Fournier, B.; Hale, W.M. Effects of moisture, temperature, and freezing and thawing on alkali-silica reaction. *ACI Mater. J.* **2018**, *115*, 575–584. [CrossRef]
37. Glinicki, M.A. Methods of qualitative and quantitative assessment of concrete air entrainment. *Cem. Wapno Beton* **2014**, *19*, 359–369.

38. Gong, F.; Takahashi, Y.; Segawa, I.; Maekawa, K. Mechanical properties of concrete with smeared cracking by alkali-silica reaction and freeze-thaw cycles. *Cem. Concr. Compos.* **2020**, *111*, 103623. [CrossRef]
39. Glinicki, M.A.; Jóźwiak-Niedźwiedzka, D.; Antolik, A.; Dziedzic, K.; Dąbrowski, M.; Bogusz, K. Diagnosis of ASR damage in highway pavement after 15 years of service in wet-freeze climate. *Case Stud. Constr. Mater.* **2022**, *17*, e01226. [CrossRef]